

Optical analysis of circuitry for respiratory rhythm in isolated brainstem of foetal mice

Kenneth J. Muller^{1,2,*}, Gavriil Tsechpenakis³, Ryota Homma^{2,4},
John G. Nicholls^{2,5}, Lawrence B. Cohen^{2,4} and Jaime Eugenin^{2,6}

¹*Department of Physiology and Biophysics and Neuroscience Program,
University of Miami School of Medicine, Miami, FL 33134, USA*

²*Marine Biological Laboratory, Woods Hole, MA 02543, USA*

³*Center for Computational Sciences (CCS), University of Miami, Coral Gables, FL 33146, USA*

⁴*Department of Physiology, Yale University School of Medicine, New Haven, CT 06520, USA*

⁵*SISSA, 34014 Trieste, Italy*

⁶*Department of Biology, Universidad de Santiago de Chile, USACH, Santiago, Chile*

Respiratory rhythms arise from neurons situated in the ventral medulla. We are investigating their spatial and functional relationships optically by measuring changes in intracellular calcium using the fluorescent, calcium-sensitive dye Oregon Green 488 BAPTA-1 AM while simultaneously recording the regular firing of motoneurons in the phrenic nerve in isolated brainstem/spinal cord preparations of E17 to E19 mice. Responses of identified cells are associated breath by breath with inspiratory and expiratory phases of respiration and depend on CO₂ and pH levels. Optical methods including two-photon microscopy are being developed together with computational analyses. Analysis of the spatial pattern of neuronal activity associated with respiratory rhythm, including cross-correlation analysis, reveals a network distributed in the ventral medulla with intermingling of neurons that are active during separate phases of the rhythm. Our experiments, aimed at testing whether initiation of the respiratory rhythm depends on pacemaker neurons, on networks or a combination of both, suggest an important role for networks.

Keywords: breathing; two-photon microscopy; calcium imaging; brainstem

1. INTRODUCTION

The rhythm of breathing, so regular and reliable, is generated by circuitry in the brainstem. While the rhythm can be controlled consciously, strengthens with exertion and with build up of carbon dioxide (and lowered pH) and is interrupted by coughing or sighing, it cannot be willed to stop altogether. Key questions remain about the neuronal source of the rhythm, its control and mechanisms for its change or plasticity (St Jacques & St John 1999; Feldman *et al.* 2003; Chatonnet *et al.* 2006; Onimaru *et al.* 2006).

It is known that the rhythm for breathing is generated in the brainstem by distributed neuronal circuitry that takes shape and begins functioning well before birth (Thoby-Brisson *et al.* 2005; Chatonnet *et al.* 2006; Thoby-Brisson & Greer 2008), although details of its functioning differ in foetuses, neonates and adults (Hilaire & Duron 1999). Thus, not only are premature human infants capable of rhythmical breathing—it may be inflation of the lungs that is limiting—but other mammals including mice also develop rhythms for breathing well before birth

(Eugenin *et al.* 2003; Onimaru & Homma 2005; Thoby-Brisson *et al.* 2005). Although post-natal development brings increasing complexity, one approach to understanding the fundamental organization of the respiratory neurons in the brainstem is to determine how they function to drive a respiratory rhythm in the developing foetus just before birth. It is experimentally useful that explants of the brainstem and spinal cord of small mammals, including mice, rats and opossums, retain the capacity for respiratory activity for hours or even days in oxygenated medium (Eugenin & Nicholls 1997, 2000; Eugenin *et al.* 2006; Kawai *et al.* 2006).

The underlying circuitry generating the breathing rhythm begins within a rostrocaudal column of cells located bilaterally in the brainstem, in the ventral medulla with additional respiratory regions in the dorsal medulla and pons. In the ventral medulla, it extends from the vicinity of the facial nucleus caudally to the spinal cord. A variety of physiological techniques, including single-unit recordings from animals, from brainstem explants and from tissue slices, have been used to try to identify neurons not only active during particular phases of the rhythm, but also whose presence is crucial for the rhythm itself (Barnes *et al.* 2007). Some of the work has focused on neurons located part way along the column at about the level of the hypoglossal nerve (Smith *et al.* 1991; Del Negro *et al.* 2002). This is in part because the hypoglossal nerve innervates the tongue, which

*Author and address for correspondence: Department of Physiology and Biophysics, University of Miami School of Medicine, Building RMSB, Room 5089, 1600 NW 10 Avenue, Miami, FL 33136, USA (kmuller@miami.edu).

One contribution of 17 to a Discussion Meeting Issue 'Brainstem neural networks vital for life'.

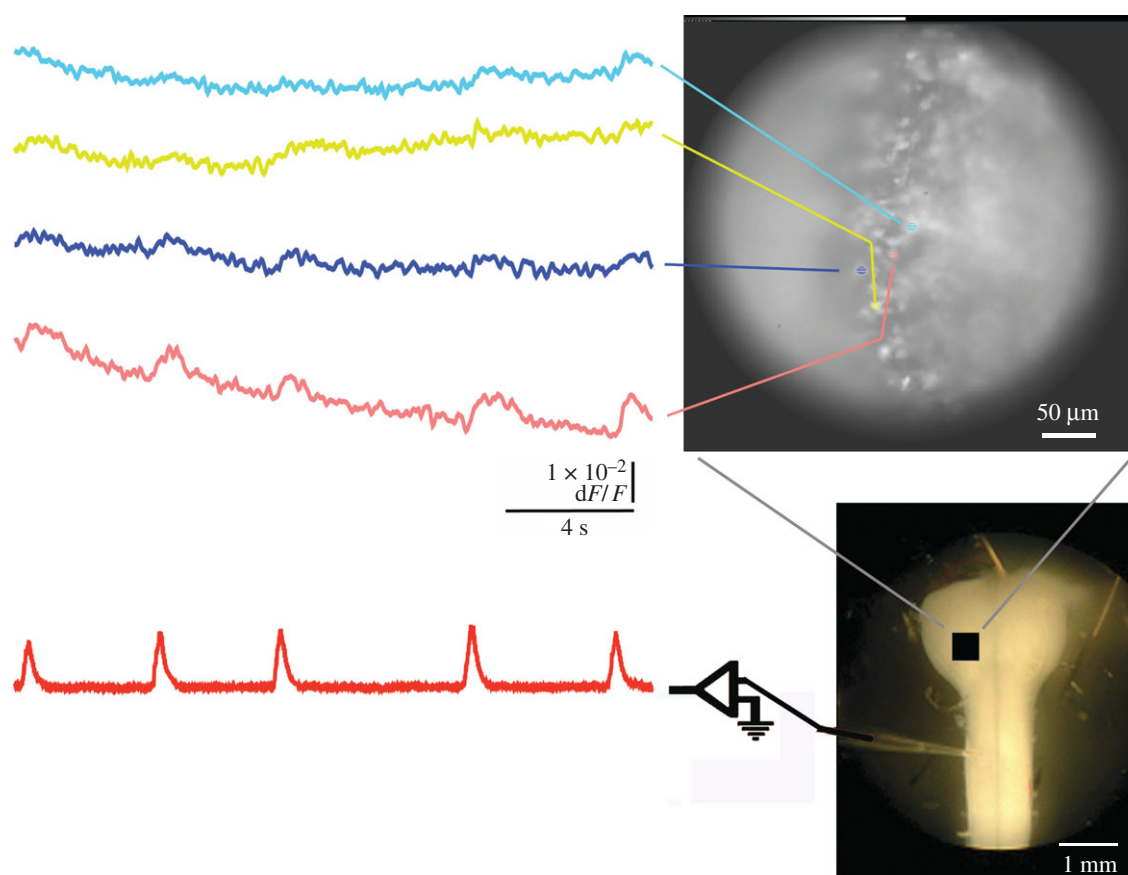


Figure 1. Recordings of fluorescence changes (top left traces) in rostral medulla (right, top and bottom) and the simultaneous integrated activity recorded from the C4 ventral root (bottom left trace) in brainstem–spinal cord preparation of E18 mouse (5% CO₂, pH 7.4) stained with Oregon Green BAPTA-1 AM, a calcium-sensitive dye, recorded optically and electrically, respectively, during a period of 20 s. Changes in fluorescence were averaged within coloured areas in the upper photograph and displayed as corresponding coloured traces on the left. A photograph of a similar preparation is shown (right, bottom) with a suction electrode attached to the ventral root and the approximate region of view indicated with a black square.

moves during respiration, permitting recording of a signal linked to the respiratory rhythm even in brain slices, but the role of the neurons in the rhythm remains unclear. What is evident from the many separate electrical recordings and from recent measurements of cellular activity using voltage- or calcium-dependent fluorescent dyes is that thousands of neurons on the left and right sides of the medulla are active in conjunction with respiration.

Although much of our understanding of the functional circuitry of the mammalian brain has come from electrophysiological recordings with single electrodes (Long & Duffin 1986; Ezure 1990; Feldman *et al.* 2003) and more recently with multi-electrode arrays (Lindsey *et al.* 2000; Segers *et al.* 2008), there is some question about the usefulness of recording respiratory rhythms from the hypoglossal nerve (St John *et al.* 2004). Optical recording techniques have the obvious advantage that the activity of many neurons can be recorded at once, preserving the spatial distribution of the different cells (Potts & Paton 2006). Each technique has limitations, and optical recordings may have lower temporal resolution than electrical recordings. But recent work using optical recording with calcium-sensitive dyes taken up by cells in the ventral brainstem of the foetal mouse while recording respiratory activity electrically from phrenic motoneurons innervating the diaphragm has provided an

opportunity to study the spatial organization and responses of respiratory neurons, breath by breath (Eugenin *et al.* 2006). The amount of data that come from optical recordings is massive and presents a challenge for analysis. Crucial for the analysis is the ability to correlate optical signals with rhythmical electrical signals of the phrenic nerve driven by the generator network in the brainstem. The aim of this paper is to use the special features of the respiratory system to devise new approaches for computational analysis of the optical and electrical data and, using two-photon confocal microscopy, to present a first step towards recording the activity of many separate respiratory neurons deeper within the medulla of the foetal mouse. The signals at deeper levels should also indicate whether diffusion of gases and nutrients affects cells deep within the medullary explant. Extensive networks in the medulla should be revealed by light microscopy.

2. METHODS

The experiments reported and reviewed here were done on foetal mice (CD1 and CF1) from embryonic day 16 to 20 at the Marine Biological Laboratory in Woods Hole, MA, USA, and at the University of Miami Medical School, Miami, FL, USA. Experiments were made as described (Eugenin *et al.* 2006), performed according to the Institute for Laboratory Animal

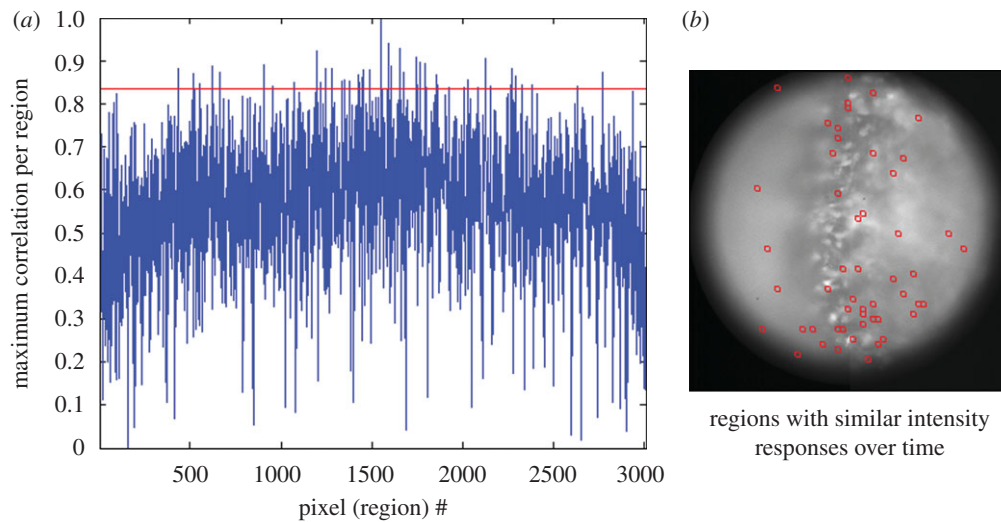


Figure 2. Analysis of cross correlation of optical and electrical signals during respiratory activity using data of figure 1. The resting light image, comprising 3000 pixels, was used to generate 3000 regions of 64 pixels, each centred on one of the pixels in the field of 3000. The intensity values for each region were obtained for 500 time points taken at 25 Hz. (a) The maximum cross correlation with the electrical signal (respiratory rhythm) is plotted for each pixel region. An arbitrarily selected value for maximum cross correlation is shown as a red line. The points above the red line in the graph are associated with pixel regions having a maximum correlation at or above the value 0.83, with those regions shown as red squares in (b). A lower value for the red line would increase the number of regions that would be selected (not shown).

Research Guide for the Care and Use of Laboratory Animals and approved by Institutional Animal Care and Use Committees at the Marine Biological Laboratory and the University of Miami. Methods for euthanasia were in agreement with the 'Report of the AVMA Panel on Euthanasia (2000)'.

In brief, explants of brainstem and attached spinal cord were taken from embryos removed by caesarean section from pregnant mothers (Charles River Laboratories Inc., Wilmington, MA, USA) under anaesthesia (ketamine/xylazine, 80/20 mg kg⁻¹ i.p.). The mothers were killed by anaesthetic overdose. Embryos were placed in 4°C artificial cerebrospinal fluid (aCSF) and killed instantaneously by removal of the heart. The aCSF contained (mM): NaCl, 125; NaHCO₃, 24; KCl, 5; CaCl₂, 1.0; MgSO₄, 1.25; KH₂PO₄, 1.25; glucose, 30; gassed and equilibrated with CO₂: O₂ = 5% : 95% (pH = 7.4). The cerebrum was removed by pontomesencephalic followed by pontobulbar transection. During some experiments, there was a shift to medium equilibrated with CO₂: O₂ = 10% : 90% (pH = 7.2) to determine chemosensitivity.

Brainstem preparations were stained with a calcium-sensitive dye, Oregon Green 488 BAPTA-1 AM (Molecular Probes, Eugene, OR, USA), either by bathing the preparation for 45–60 min as described (Eugenin *et al.* 2006) for observation with conventional fluorescence microscopy or by injection of a solution (2.5 µg µl⁻¹) extracellularly up to 400 µm beneath the ventral surface of the central nervous system for experiments using a Zeiss LSM 510 two-photon microscope operating at 800 nm fitted with a Zeiss 20× 1.0 NA water immersion objective provided by the Marine Biological Laboratory. Electrical signals were simultaneously obtained from a C3–C5 ventral root as described (Eugenin *et al.* 2006) and recorded with NEUROPLEX software (RedShirtImaging, LLC, Decatur, GA, USA), which combined electrical signals

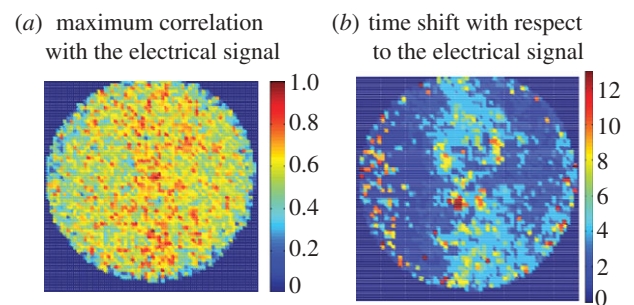


Figure 3. (a) The maximum cross correlation with the electrical signal for each pixel region is displayed in colour, showing the strongest correlation with approximately the same distribution as shown for the red squares in figure 2. (b) The time used to obtain each maximum cross correlation between the electrical and optical signals in (a) is displayed in (b) using pseudocolour to indicate the delay or time shift.

of integrated activity and optical signals initially recorded with Zeiss Zen 2008 software. Acquisition trials were generally 20 s in length with images taken typically at 25 ms intervals using conventional fluorescence microscopy and at 250 ms intervals using two-photon microscopy. Data analysis was done both with NEUROPLEX and with software custom-designed by one of us (G.T.).

To analyse the patterns between the electrical and the optical signals, separate approaches were used for (i) widefield and (ii) two-photon fluorescence microscopy. (i) For widefield microscopy for the intensity (optical) signals, we used the average intensity within regions of pre-defined size, centred at every pixel of the images of the acquired stack. The advantage of using intensity from the entire image field is that we avoided manual sampling, and therefore we could obtain detailed results for the entire field of view over time. A potential drawback of this approach

is that we also obtain a large number of intensity signals (over time) that do not correspond to cell regions and, therefore, are not informative in our analysis; furthermore, these non-informative signals can bias our analysis (as 'noise') if we do not use robust methods for the pattern analysis. One of the most fundamental measurements of the similarity between the two signals is the cross correlation, and from digital signal processing theory, it is one of the most robust. If one signal is time shifted with respect to the other (time delay), cross correlation provides information about this delay, i.e. the time shift at which the two signals have the maximum correlation. Also, in this analysis, we can use the raw signals without temporal filtering. (ii) As a first step for two-photon microscopy, in which single cells were imaged, processed image differences were taken. Thus, the optical signals were spatially and temporally filtered, and the differences between ratioed optical signals that had been recorded at particular phases of the respiratory rhythm were displayed in pseudocolour to identify for further analysis those cells showing changes in fluorescence that correlated with particular phases of the respiratory rhythm. The subtractions were done using NEUROPLEX software. Homma *et al.* (2009) in this issue further describe this approach.

3. RESULTS

(a) *Optical recording from respiratory regions of the ventral medulla while electrically recording respiratory activity from ventral roots*

Respiratory neurons in the brainstem are situated near the ventral surface, making them more accessible to bath-applied calcium-sensitive dyes such as Oregon Green BAPTA-1 AM that are taken up by cells. This is particularly so in the smaller foetus, in which glia are sparse and distances to the surface are shorter. Since increased neuronal activity is associated with Ca^{2+} signals that arise primarily from neuronal cell bodies and the axon initial segment region (Ross 1989; Przywara *et al.* 1991), signals are expected to be predominantly from cell bodies. In fact, we have reported (Eugenin *et al.* 2006) and here confirm the rhythmical fluorescence signal generated by dye-stained cells in the ventral medulla (figure 1) during the corresponding electrical activity of the respiratory rhythm recorded from spinal motoneurons that innervate the diaphragm. In figure 1, the brainstem is in clearest focus along a line of stained cells near the surface that happens to be the vertical axis, while cells farther beneath the surface to the right in the field of view are less distinct. The left side of the image is focused above the surface of the brainstem and therefore has no distinct cells. The optical recordings show that the activity is spatially distributed but not uniform, reflecting the organization of the respiratory network in the brainstem. The previously reported experiments showed that optically measured activity became stronger and faster, in accord with separate electrical measurements using extracellular microelectrodes in corresponding regions of the brainstem, when CO_2 levels were increased from 5 to 10 per cent or when pH dropped from 7.4 to 7.2 (Eugenin *et al.* 2006).

(b) *Analysis and cross correlation of medullary optical and spinal cord electrical signals during respiratory rhythm*

Key problems include how best to analyse the optical signal and determine whether there are distinctly different regions within the field of view, and whether the timing and spatial extent of activity can be described as a pattern with respect to the spinal electrical signal associated with respiration. Homma *et al.* (2009) in this issue describe one approach, using subtraction of fluorescence signals linked to particular phases of the respiratory rhythm, which is described in the following in conjunction with two-photon fluorescence recording for identifying rhythmogenic regions. It uses commercial NEUROPLEX software.

Another approach, presented here for the widefield data, was to begin by analysing the image pixel by pixel and frame by frame, averaging the signal in 64 pixel arrays centred on each pixel to obtain an average intensity for each region, which was then plotted over time. At the magnification used, each pixel was 1.4 μm . Next, for each pixel region (i.e. the group of 64 pixels centred on a particular pixel), the cross correlation between the optical signal for that region and the integrated electrical signal was determined, with the aim of identifying those regions whose optical activity best correlated with the electrical signal. Such an analysis is shown in figure 2(a), where the graph displays as its abscissa the complete set of pixel regions and the ordinate is the maximum or best correlation for each of those regions. The points above the arbitrarily selected red line at 0.83 in the graph indicate pixel regions with a maximum correlation at or above the value for the red line, with those regions shown as red squares in figure 2(b). Lowering the value of the red line would increase the number of regions appearing in figure 2(b). This indicates some correlation for many points. The 'noise level' is shown for the region outside the circle, below 0.2. The regions with the highest correlation, whether phase shifted or not, are concentrated in the region that is closest to the surface of the brain along a line that approximately bisects the figure. But, there are many regions particularly deeper in the brainstem that exhibit a highly correlated signal. The overall distribution is shown in figure 3a, where the maximum correlation for each pixel region is displayed in pseudocolour, and the result is similar to that shown in figure 2.

The respiratory neurons in the ventral medulla have been characterized according to the phase of the respiratory rhythm during which they have peak activity, whether inspiratory, as in the example of figure 1, or expiratory or pre-inspiratory. To identify areas of the image that have pixel regions or clusters that exhibit particular phases, it is useful to graph or display the time shift required for maximum correlation between the optical and electrical signals. For the image of figures 1–3, this is displayed as figure 3b, in which the higher numbers represent a greater shift. Since the sampling rate was 25 Hz, the maximum shift (red) is approximately 0.5 s. Because all points are shown, without regard to the strength of correlation,

there are not only phase-shifted pixels along the centre, where regional differences in phase are evident, but also along the left margin, where the cross correlation is relatively low, so that there the shifted regions represent noise. Having such a region gives credence to the results that show little phase shift over a larger region.

(c) *Imaging of single neurons within the brainstem*

In images like those in figure 1 that are typical of recordings with conventional widefield fluorescence microscopy, it appears that the calcium-sensitive dye is capable of staining and revealing single cells. In fact, some respiratory-related signals seem to come from regions that coincide with the staining and appear to be cells. But, conventional fluorescence microscopy after bath application of dye, with its lack of depth resolution, leaves open the question of whether single neurons provide the signals that are being recorded and whether neurons deep below the surface are active. To address these questions and to examine the depth and distribution of respiratory neurons in the ventral medulla, as well as the relationships between those neurons, the experiments performed with conventional microscopy were repeated using a two-photon microscope, with results shown in figure 4. Prior to recording, Oregon Green BAPTA-1 AM dye was injected in those regions that extracellular recording and earlier optical recordings had indicated were likely to be sites of respiratory neurons, such as the region shown in black superimposed upon a photo of an example of the preparation used. Strong respiratory signals were recorded optically from close to the surface to depths of more than 200 μm , although for best signal intensity recordings were not usually made deeper.

In figure 4, the three photographic panels above the diagram of a brainstem–spinal cord preparation show the field sampled at 4 Hz during 20 s, which was a region 350 μm \times 175 μm . The images in the three panels are displayed at 25 per cent of the original spatial resolution. On the left are optical signals taken from four small regions (marked by coloured hatching), the approximate size of cell bodies, shown in the middle and top panels. These correspond to four cells with visible resting fluorescence in the same, unlabelled micrograph in the bottom panel displaying resting fluorescence. The integrated electrical recording from the ventral root at C4 is displayed in red in the lower left portion of figure 4, sampled at 100 Hz, and aligned with the coloured traces above showing concurrent optical traces of the responses of the four coloured regions in the micrographs. The peaks in the electrical recording mark bursts of phrenic motoneuron activity associated with inspiration; dark blue and red bars, marked 1 and 2, respectively, show the timing of frames used to generate the difference image displayed in pseudocolour in the upper right panel. In that panel, the greatest inspiratory responses relative to the signals preceding it appear in red; optical signals that peak during inspiratory activity typically include cells that appear orange or

red in the difference image, as shown, whereas cells such as that marked in blue had optical signals with little or no respiratory rhythm.

By creating such difference images for each peak of the electrical signal, corresponding to each breath, overlapping but not identical sets of cells with peak optical responses can be identified (not shown), reflecting individual variability in the cellular responses as suggested by the differences between the turquoise, yellow and violet traces shown in figure 4. Although the relationship between optical signals and electrical firing of cells remains unknown, the observation is in agreement with our finding cellular differences and ‘failures’ in responses recorded with extracellular microelectrodes during respiratory activity (Eugenin *et al.* 2006).

4. DISCUSSION

In this and our other recent work (Eugenin *et al.* 2006), it has been shown that optical recording of activity from the ventral aspect of the foetal mouse brainstem can identify respiratory neurons that are active during the respiratory cycle as recorded from spinal motoneurons. The locations that have been identified previously as containing neurons of the respiratory pattern generator are the same locations that produce the optical signal. Our published recordings have shown that inspiratory, expiratory and pre-inspiratory optical signals are intermingled but separate (Eugenin *et al.* 2006). Furthermore, when the extracellular bathing solution is changed to lower pH or higher CO₂ concentration, the respiratory rhythm becomes faster and the signals from different regions become more similar, without the failures and reduced signals that are evident in separate traces produced by different regions (Eugenin *et al.* 2006).

The introduction of two-photon microscopy has immediately answered several questions that were raised using conventional, widefield fluorescence microscopy and has shown that substantial activity could be recorded from single cells deep beneath the surface. First, it is evident that signals are coming from neuronal cell bodies, as previously assumed. Although some respiratory cells are present at depths of at least 200 μm below the surface, others are within one or two cell diameters of the surface and are stained by bath application of dye. Recent histological studies by one of us (Eugenin *et al.* 2008) has confirmed that there are few glia present in the mouse brainstem at post-natal day 1, which strongly suggests that the cells that are stained and giving signals are certainly neurons and not glia.

The large amount of data generated by the optical experiments makes the automated analysis suggested and outlined in the present paper particularly welcome. In addition, the analysis removes potential bias and offers an alternative view of the results of the experiments compared with that published previously. By expanding the use of the cross correlations, it will be possible to determine the inter-relationships of cells or regions that respond best

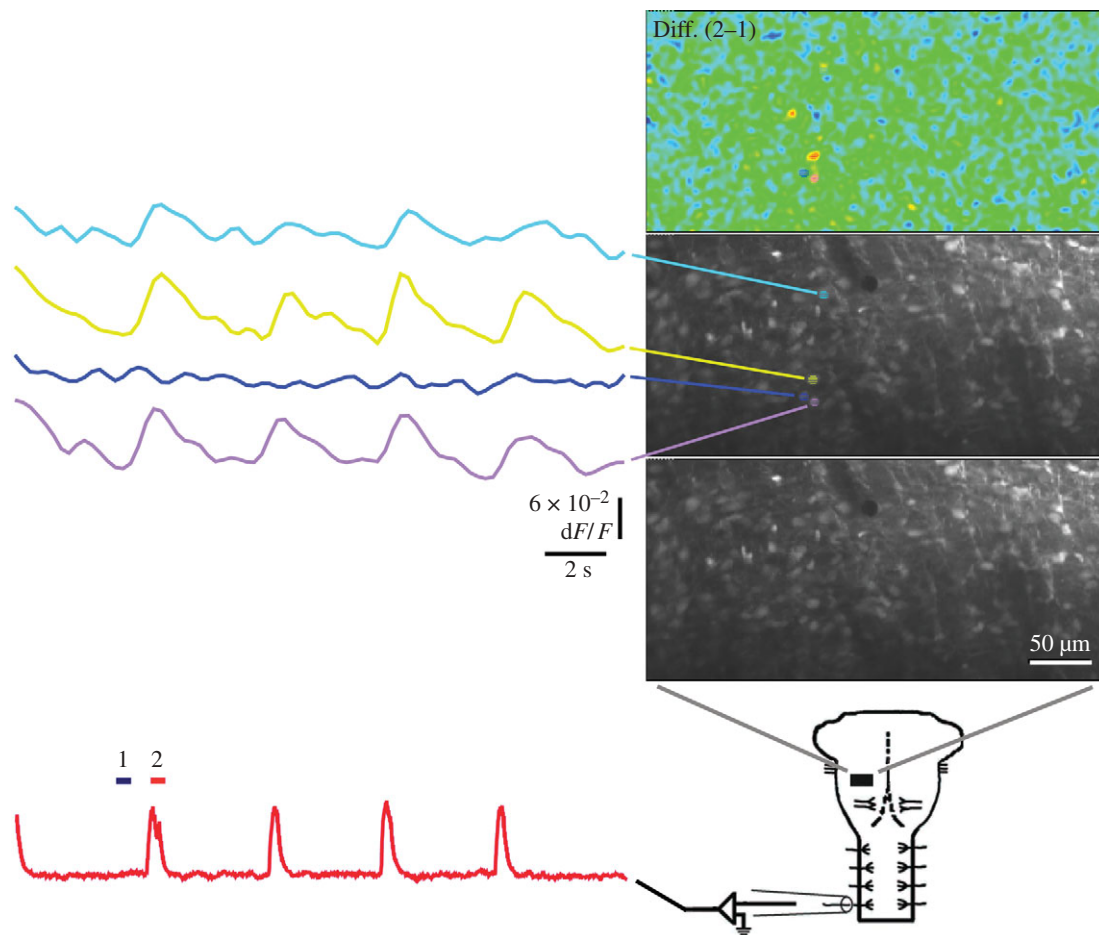


Figure 4. Optical recordings using a two-photon microscope of fluorescence changes linked to the electrically recorded respiratory rhythm from an E18 mouse. Relative fluorescence changes are shown in coloured traces on the left for corresponding regions in images on the right. The bottom left trace shows the simultaneous integrated activity recorded with a suction electrode from the C4 ventral root in brainstem–spinal cord preparation of E18 mouse. The typical preparation as in figure 1, shown in diagram at bottom right, was viewed at various depths in a field that was usually $350\ \mu\text{m} \times 175\ \mu\text{m}$, indicated by the black rectangle, which corresponds to the three images above it. The region under observation was injected with Oregon Green BAPTA-1 AM, a calcium-sensitive dye, recorded optically and electrically during a period of 20 s. The lowest image shows the ‘resting’ fluorescence signal, with the cell bodies all appearing to have taken up dye. The middle image is the same except for the overlay, corresponding to four cells, which shows four regions in separate colours for which the optical signals are displayed at the left. The simultaneously recorded electrical signal obtained by integrating the activity of the phrenic nerve in the C4 ventral root shows peaks during what would be inspiration. The bars corresponding to two images sampled before (dark blue, 1) and during (red, 2) the first full peak indicate the timing of images that were averaged and then the two pairs subtracted to produce the pseudocolour difference image (Diff. (2–1)), which was both temporally and spatially averaged. The yellow and red regions indicate regions of greatest change, corresponding to cells with fluorescence changes linked to the respiratory rhythm, as shown, whereas the blue cell that did not have such a signal is typical of cells that can be neighbours of those having signals that have no activity linked to the rhythm. Some neighbours may display signals that are not linked to the rhythm.

during different phases of the rhythm or that respond similarly but are spatially separate. Automated analysis will be able to identify functionally linked cells or regions.

Experiments in the future will be done to perturb the activity of specific cells or cell groups to be able to identify functional connectivity and the roles of cells in the generation of the rhythm. By combining experiment with automated analysis, it will be possible to determine whether cells that appear to contribute to particular phases of the rhythm are preferentially affected and whether inhibitory as well as excitatory connections are present. The laser may permit focal ablation or stimulation of particular neurons, so that

local interactions might be mapped using two-photon laser microscopy.

There is now an opportunity for simultaneous optical recording from many distributed components of the respiratory generator in the foetal mouse brainstem together with electrical recordings from the spinal output of that generator. With a range of computational tools, it is now possible to analyse those distributed components and prepare to test their function in the generator circuitry by targeted application of drugs and focal excitation and ablation with the laser.

Professor Bruce G. Lindsey participated in the experiments. Supported by FONDECYT 1060110 (J.E).

REFERENCES

- Barnes, B. J., Tuong, C. M. & Mellen, N. M. 2007 Functional imaging reveals respiratory network activity during hypoxic and opioid challenge in the neonate rat tilted sagittal slab preparation. *J. Neurophysiol.* **97**, 2283–2292. (doi:10.1152/jn.01056.2006)
- Chatonnet, F., Borday, C., Wrobel, L., Thoby-Brisson, M., Fortin, G., McLean, H. & Champagnat, J. 2006 Ontogeny of central rhythm generation in chicks and rodents. *Respir. Physiol. Neurobiol.* **154**, 37–46. (doi:10.1016/j.resp.2006.02.004)
- Del Negro, C. A., Koshiya, N., Butera Jr, R. J. & Smith, J. C. 2002 Persistent sodium current, membrane properties and bursting behavior of pre-Bötzinger complex inspiratory neurons *in vitro*. *J. Neurophysiol.* **88**, 2242–2250. (doi:10.1152/jn.00081.2002)
- Eugenin, J. & Nicholls, J. G. 1997 Chemosensory and cholinergic stimulation of fictive respiration in isolated CNS of neonatal opossum. *J. Physiol. (Lond.)* **501**, 425–437. (doi:10.1111/j.1469-7793.1997.425bn.x)
- Eugenin, J. & Nicholls, J. G. 2000 Control of respiration in the isolated central nervous system of the neonatal opossum, *Monodelphis domestica*. *Brain Res. Bull.* **53**, 605–613. (doi:10.1016/S0361-9230(00)00394-4)
- Eugenin, J., Ampuero, E., Infante, C. D., Silva, E. & Llona, I. 2003 pH sensitivity of spinal cord rhythm in foetal mice *in vitro*. *Adv. Exp. Med. Biol.* **536**, 535–539.
- Eugenin, J., Nicholls, J. G., Cohen, L. B. & Muller, K. J. 2006 Optical recording from respiratory pattern generator of foetal mouse brainstem reveals a distributed network. *Neuroscience* **137**, 1221–1227. (doi:10.1016/j.neuroscience.2005.10.053)
- Eugenin, J., Otarola, M., Bravo, E., Coddou, C., Cerpa, V., Reyes-Parada, M., Llona, I. & von Bernhardi, R. 2008 Prenatal to early postnatal nicotine exposure impairs central chemoreception and modifies breathing pattern in mouse neonates: a probable link to sudden infant death syndrome. *J. Neurosci.* **28**, 13 907–13 917. (doi:10.1523/JNEUROSCI.4441-08.2008)
- Ezure, K. 1990 Synaptic connections between medullary respiratory neurons and considerations on the genesis of respiratory rhythm. *Prog. Neurobiol.* **35**, 429–450. (doi:10.1016/0301-0082(90)90030-K)
- Feldman, J. L., Mitchell, G. S. & Nattie, E. E. 2003 Breathing: rhythmicity, plasticity, chemosensitivity. *Ann. Rev. Neurosci.* **26**, 239–266. (doi:10.1146/annurev.neuro.26.041002.131103)
- Hilaire, G. & Duron, B. 1999 Maturation of the mammalian respiratory system. *Physiol. Rev.* **79**, 325–360.
- Homma, R., Baker, B. J., Jin, L., Garaschuk, O., Konnerth, A., Cohen, L. B. & Zecevic, D. 2009 Wide-field and two-photon imaging of brain activity with voltage- and calcium-sensitive dyes. *Phil. Trans. R. Soc. B* **364**, 2453–2467. (doi:10.1098/rstb.2009.0084)
- Kawai, A., Onimaru, H. & Homma, I. 2006 Mechanisms of CO₂/H⁺ chemoreception by respiratory rhythm generator neurons in the medulla from newborn rats *in vitro*. *J. Physiol.* **572**, 525–537. (doi:10.1113/jphysiol.2005.102533)
- Lindsey, B. G., Morris, K. F., Segers, L. S. & Shannon, R. 2000 Respiratory neuronal assemblies. *Respir. Physiol.* **122**, 183–196. (doi:10.1016/S0034-5687(00)00158-4)
- Long, S. & Duffin, J. 1986 The neuronal determinants of respiratory rhythm. *Prog. Neurobiol.* **27**, 101–182. (doi:10.1016/0301-0082(86)90007-9)
- Onimaru, H. & Homma, I. 2005 Developmental changes in the spatio-temporal pattern of respiratory neuron activity in the medulla of late foetal rat. *Neuroscience* **131**, 969–977.
- Onimaru, H., Kumagawa, Y. & Homma, I. 2006 Respiration-related rhythmic activity in the rostral medulla of newborn rats. *J. Neurophysiol.* **96**, 55–61. (doi:10.1152/jn.01175.2005)
- Potts, J. T. & Paton, J. F. 2006 Optical imaging of medullary ventral respiratory network during eupnea and gasping *in situ*. *Eur. J. Neurosci.* **23**, 3025–3033. (doi:10.1111/j.1460-9568.2006.04809.x)
- Przywara, D. A., Bhave, S. V., Bhave, A., Wakade, T. D. & Wakade, A. R. 1991 Stimulated rise in neuronal calcium is faster and greater in the nucleus than the cytosol. *FASEB J.* **5**, 217–222.
- Ross, W. N. 1989 Changes in intracellular calcium during neuron activity. *Ann. Rev. Physiol.* **51**, 491–506. (doi:10.1146/annurev.ph.51.030189.002423)
- Segers, L. S., Nuding, S. C., Dick, T. E., Shannon, R., Baekey, D. M., Solomon, I. C., Morris, K. F. & Lindsey, B. G. 2008 Functional connectivity in the ponto-medullary respiratory network. *J. Neurophysiol.* **100**, 1749–1769. (doi:10.1152/jn.90414.2008)
- Smith, J. C., Ellenberger, H. H., Ballanyi, K., Richter, D. W. & Feldman, J. L. 1991 Pre-Bötzinger complex: a brainstem region that may generate respiratory rhythm in mammals. *Science* **254**, 726–729. (doi:10.1126/science.1683005)
- St Jacques, R. & St John, W. M. 1999 Transient, reversible apnoea following ablation of the pre-Botzinger complex in rats. *J. Physiol. (Lond.)* **520**, 303–314. (doi:10.1111/j.1469-7793.1999.00303.x)
- St John, W. M., Paton, J. F. & Leiter, J. C. 2004 Uncoupling of rhythmic hypoglossal from phrenic activity in the rat. *Exp. Physiol.* **89**, 727–737. (doi:10.1113/expphysiol.2004.028829)
- Thoby-Brisson, M. & Greer, J. J. 2008 Anatomical and functional development of the pre-Botzinger complex in prenatal rodents. *J. Appl. Physiol.* **104**, 1213–1219. (doi:10.1152/jappphysiol.01061.2007)
- Thoby-Brisson, M., Trinh, J.-B., Champagnat, J. & Fortin, G. 2005 Emergence of the pre-Bötzinger respiratory rhythm generator in the mouse embryo. *J. Neurosci.* **25**, 4307–4318. (doi:10.1523/JNEUROSCI.0551-05.2005)